Table 1 Average error for test cases 1–4

	Case 1, $t = 1.5$		Case 2, $t = 1.5$		Case 3, $t = 2$		Case 4, $t = 2$	
$\Delta x, \Delta t$	0.025	0.0625	0.025	0.0625	0.025	0.0625	0.025	0.0625
$\omega = 3$	0.1248	0.2331	0.0146	0.0819	0.1820	0.2466	0.0609	0.1851
$\omega = c^2(4-c^2)$	0.1019	0.1972	0.0029	0.0380	0.1411	0.2618	0.0215	0.1183

Table 2 Definition of test cases 5–8

Case	$\phi_1(0,x)$	$\phi_2(0,x)$	a_1	b_1	a_2	b_2
Case 5	$H(x-\frac{1}{2})$	$\cos^2\pi(x-\frac{1}{4})$	1.05	0.9	2.5	1
Case 6	$\sin^2\pi x$	$\cos^2\pi(x-\frac{1}{4})$	1.05	0.9	2.5	1
Case 7	$H(x-\frac{1}{2})$	$\cos^2\pi(x-\frac{1}{4})$	1.4	0.2	2.8	0.4
Case 8	$\sin^2\pi x$	$\cos^2\pi(x-\frac{1}{4})$	1.4	0.2	2.8	0.4

Table 3 Average error for test cases 5–8

Damping term		Case 5, $t = 3$		Case 6, $t = 3$		Case 7, $t = 3$		Case 8, $t = 3$	
	$\Delta x, \Delta t$	0.025	0.0625	0.025	0.0625	0.025	0.0625	0.025	0.0625
Eq. (5)	ε_1	0.1056	0.2241	0.0023	0.0383	0.0913	0.1868	0.00095	0.0118
	ε_2	0.0268	0.0405	0.0038	0.0428	0.0322	0.0390	0.00107	0.0155
Eq. (10)	ε_1	0.1032	0.2157	0.0025	0.0394	0.0610	0.1866	0.000092	0.0036
	ε_2	0.0314	0.0663	0.0022	0.0288	0.0150	0.0303	0.000081	0.0027

where ψ_k is the kth component of the vector $\psi = U\phi$. For optimum accuracy ω should satisfy $\omega = c_k^2(4-c_k^2)$, with $c_k = \sigma|\lambda_k|$, where λ_k is the kth eigenvalue of F. However, stability requires $\omega \geqq c_m^2(4-c_m^2)$, which is larger than $c_k^2(4-c_k^2)$, except for the value of k which corresponds to the absolutely largest eigenvalue. The $(n-1)$ unknowns with a different value of k are evaluated with possibly strongly diminished accuracy.

However, it is possible to obtain optimum accuracy for all components simultaneously, if the scalar ω is replaced by the matrix Ω, defined as

$$\Omega = C^2(4I - C^2) \tag{9}$$

with $C = \sigma\Lambda$ and I the identity matrix. The damping term in Eq. (5) is then found to be

$$D = -\tfrac{1}{24}\delta^4 d_j^n, \qquad d = U^{-1}\Omega U\phi \tag{10}$$

Replacement of Eq. (5) by Eq. (10) conserves the third order accuracy of the RBM scheme, because the difference between Eqs. (5) and (10) is of fourth order. The predictor-corrector form is also preserved, because the matrix multiplications necessary to obtain d may be done analytically beforehand. For this the eigenvalues and the diagonalizing matrix of F are needed. These may be considered known, because in applications they are necessary for a good understanding of the phenomenon under study. Replacement of Eq. (5) by Eq. (10) makes the RBM scheme slightly more time-consuming, because in addition to the function evaluations necessary to determine f^n, $f^{(1)}$, and $f^{(2)}$ an additional function evaluation to determine d is necessary.

The considerable increase in accuracy which one may expect from replacing Eq. (5) by Eq. (10) is demonstrated by the following example:

$$F = \begin{pmatrix} c_1 & c_2 \\ c_2 & c_1 \end{pmatrix}, \quad \begin{aligned} c_{1,2} &= (\lambda_1 \pm \lambda_2)/2 \\ \lambda_{1,2} &= (a_{1,2} + b_{1,2}\cos^2\pi x)^{-1} \end{aligned} \tag{11}$$

If $\phi(0,x)$ is periodic in x with period 1 and $a_1 + \frac{1}{2}b_1 = p$, $a_2 + \frac{1}{2}b_2 = np$, where n is an integer, the exact solution is periodic in t with period np.

The four cases that were calculated are listed in Table 2. The average error in ϕ_1 and ϕ_2, called ε_1 and ε_2, respectively, is defined as in Eq. (7) and listed in Table 3. The results confirm that with the damping term D defined by Eq. (10) the RBM scheme is considerably more accurate than with D defined by Eq. (5), especially when the solution is smooth.

References

[1] Richtmyer, R. D. and Morton, K. W., *Difference Methods for Initial-Value Problems*, 2nd ed., Interscience, New York, 1967, p. 303.

[2] Rusanov, V. V., "Difference Schemes of the Third Order of Accuracy for Continuous Computation of Discontinuous Solutions," *Soviet Math. Dokl.*, Vol. 9, 1968, pp. 771–774.

[3] Burstein, S. Z. and Mirin, A. A., "Third Order Difference Methods for Hyperbolic Equations," *Journal of Computational Physics*, Vol. 5, 1970, pp. 547–571.

[4] Rusanov, V. V., "On Difference Schemes of Third Order Accuracy for Nonlinear Hyperbolic Systems," *Journal of Computational Physics*, Vol. 5, 1970, pp. 507–516.

An Automated Gradient Projection Algorithm for Optimal Control Problems

STANLEY G. RAJTORA* AND BION L. PIERSON†

Iowa State University, Ames, Iowa

Introduction

ONE method of treating optimal control problems with terminal state constraints is to adjoin these constraints to

Received January 4, 1972; revision received February 24, 1972. This work was supported by the Engineering Research Institute, Iowa State University, Ames, Iowa.

Index category: Navigation, Control, and Guidance Theory.

* Graduate Assistant, Department of Aerospace Engineering.

† Assistant Professor, Department of Aerospace Engineering and the Engineering Research Institute. Member AIAA.

the cost functional as penalty functions and then to solve a sequence of unconstrained problems which approximates the constrained problem. This process, however, retards the convergence properties of the algorithm which is being employed. This phenomenon is similar to that occurring in parameter optimization problems for which a clear geometrical interpretation[1] can be given. An additional complication is having to estimate a value for the initial penalty constant.

Sinnott and Luenberger[2] have adapted a projection technique to a conjugate gradient algorithm in order to satisfy terminal state constraints. Although this technique avoids the undesirable characteristics of the penalty function approach, it unfortunately introduces two critical stepsize parameters which must be chosen by the user. This Note proposes using a one-dimensional minimization as an automated means of selecting the more troublesome of these two stepsize parameters. Adoption of this technique is supported by numerical results and by theoretical implications.

Projection Operator Formulation

Consider the problem of determining the r-vector of control functions $\mathbf{u}(t)$, $t_0 \leqq t \leqq t_f$, which minimizes the cost functional

$$J = \phi[\mathbf{x}(t_f)] + \int_{t_0}^{t_f} L(\mathbf{x}, \mathbf{u}, t)\, dt \tag{1}$$

subject to the nth-order nonlinear dynamical system

$$\dot{\mathbf{x}}(t) = \mathbf{f}(\mathbf{x}, \mathbf{u}, t), \qquad \mathbf{x}(t_0) = \mathbf{x}_0 \tag{2}$$

with $\mathbf{x}_0$, t_0, and t_f given, and subject to the p ($p \leqq n$) terminal state constraints

$$\boldsymbol{\psi}[\mathbf{x}(t_f)] = \mathbf{0} \tag{3}$$

Linearization of the dynamics (2) about a nominal $\mathbf{u}(t)$ and $\mathbf{x}(t)$ gives

$$\delta\dot{\mathbf{x}} = f_x(\mathbf{x}, \mathbf{u}, t)\,\delta\mathbf{x}(t) + f_u(\mathbf{x}, \mathbf{u}, t)\,\delta\mathbf{u}(t), \qquad \delta\mathbf{x}(t_0) = \mathbf{0} \tag{4}$$

for which

$$\delta\mathbf{x}(t) = \int_{t_0}^{t} \Phi(t, \tau) f_u(\tau)\, \delta\mathbf{u}(\tau)\, d\tau \tag{5}$$

where $\Phi(t, \tau)$ is the transition matrix of linear system (4), f_x and f_u are matrices with elements $\partial f_i/\partial x_j$, and $\partial f_i/\partial u_j$, respectively, and $\delta\mathbf{u}$ and $\delta\mathbf{x}$ represent variations of the control and state vectors, respectively. In addition, if each element of the vector $\boldsymbol{\psi}[\mathbf{x}]$ is differentiable and if each iteration in the process satisfies Eq. (3), then near a nominal $\mathbf{x}(t_f)$,

$$\psi_x \delta\mathbf{x} \cong \boldsymbol{\psi}[\mathbf{x} + \delta\mathbf{x}] - \boldsymbol{\psi}[\mathbf{x}] = \mathbf{0} \tag{6}$$

Combining Eq. (5) with Eq. (6) yields

$$\int_{t_0}^{t_f} \psi_x \Phi(t_f, \tau) f_u(\tau)\, \delta\mathbf{u}(\tau)\, d\tau = \mathbf{0} \tag{7}$$

For convenience, let the $p \times r$ time-varying matrix $\xi(\tau)$ be defined by $\xi(\tau) = \psi_x \Phi(t_f, \tau) f_u(\tau)$, so that Eq. (7) becomes

$$\int_{t_0}^{t_f} \xi(\tau)\, \delta\mathbf{u}(\tau)\, d\tau = \mathbf{0} \tag{8}$$

The unique[3] projection $\delta\tilde{\mathbf{u}}$ of the control variation $\delta\mathbf{u}$ onto the linearized constraint surface (8) is given by[2,4]

$$\delta\tilde{\mathbf{u}}(t) = \delta\mathbf{u}(t) - \xi^T(t)\left[\int_{t_0}^{t_f} \xi(t)\xi^T(t)\, dt\right]^{-1} \int_{t_0}^{t_f} \xi(t)\, \delta\mathbf{u}(t)\, dt \tag{9}$$

Thus, if the nominal control $\mathbf{u}$ satisfies the constraints (3), the control $\mathbf{u} + \delta\tilde{\mathbf{u}}$ satisfies the linearized constraint (6). The inverse matrix in Eq. (9) exists if the linear system (4) is controllable.

The variation of the cost functional due to $\delta\tilde{\mathbf{u}}$ is

$$\delta J = \int_{t_0}^{t_f} \tilde{H}_u\, \delta\tilde{\mathbf{u}}\, dt \tag{10}$$

where H_u is the gradient of the Hamiltonian $H = L + \boldsymbol{\lambda}^T\mathbf{f}$ with respect to the control. The vector $\boldsymbol{\lambda}(t)$ is determined by the system $\dot{\boldsymbol{\lambda}}^T(t) = -L_x - \boldsymbol{\lambda}^T f_x$ and $\boldsymbol{\lambda}^T(t_f) = \phi_x$. For an extremum, δJ must be zero for arbitrary $\delta\tilde{\mathbf{u}}(t)$; this can happen only if $\tilde{H}_u = \mathbf{0}$, for $t_0 \leqq t \leqq t_f$. If θ_i and $\mathbf{p}_i(t)$ represent the stepsize and direction of search, respectively, then $\mathbf{u}_{i+1} = \mathbf{u}_i + \theta_i \mathbf{p}_i$, so that letting $\mathbf{p}_i = -\tilde{H}_{u_i}{}^T$ insures that δJ is negative.

Stepsize Selection

One method of implementing the projection operator[2] is to: 1) choose θ_i such that $J[\mathbf{u}_i(t) + \theta_i \mathbf{p}_i(t)]$, as a function of θ_i, is a minimum; 2) let

$$\hat{\mathbf{u}}_{i+1}(t) = \mathbf{u}_i(t) + m_i \theta_i \mathbf{p}_i(t) \tag{11}$$

3) let $\boldsymbol{\psi}_i = \boldsymbol{\psi}[\hat{\mathbf{x}}(t_f)]$, where $\hat{\mathbf{x}}(t_f)$ corresponds to $\hat{\mathbf{u}}_{i+1}(t)$; 4) let

$$\Delta\mathbf{u}(t) = -\xi^T(t)\left[\int_{t_0}^{t_f} \xi(t)\xi^T(t)\, dt\right]^{-1} \boldsymbol{\psi}_i$$

and 5) let

$$\mathbf{u}_{i+1}(t) = \hat{\mathbf{u}}_{i+1}(t) + n_i \Delta\mathbf{u}(t) \tag{12}$$

If constraints (3) are not satisfied, parameters m_i and n_i are chosen so that a) $\|\boldsymbol{\psi}\|$ decreases at each step, where $\|\ \|$ is some suitable norm, and b) the performance index J decreases at each step. If $\|\boldsymbol{\psi}\| < \varepsilon$ for some $\varepsilon > 0$, the constraint is considered satisfied and motion takes place along the constraint surface. Although the intent of these steps is clear, the implementation of them is not straightforward.

Mehra and Bryson[5] and Willoughby[6] suggest that the parameter m_i in Eq. (11) in proceeding "parallel" to the constraints, can be determined by insuring that the constraint violation at the beginning and end of the step are not significantly different, i.e., the linearization has not been violated. Similarly, a linearization check is made on correction step (12) by comparing the actual constraint variation $\boldsymbol{\psi}(\mathbf{x} + \delta\mathbf{x}) - \boldsymbol{\psi}(\mathbf{x})$ to the quantity $\psi_x \delta\mathbf{x}(t_f)$, where $\delta\mathbf{x}(t_f)$ is the result of integrating the linear system (4). The parameter n_i is reduced from unity if there is a significant difference between these two quantities. This method of stepsize selection, although reasonable and well defined, does not provide full utilization of each step in the iteration process.

Willoughby[6] presents a different method of determining the elusive scalar m_i in which m_i is reduced from unity only if: 1) the correction in Eq. (12) leads to greater rather than smaller constraint violation, or 2) the value of the cost functional after correcting the control in Eq. (12) increases. He found that this criterion does, at least for the test case solved, lead to a better convergence history than the method first described, since larger stepsizes are taken. It was this increase in performance, due to the increased stepsize, which initially motivated the following stepsize selection technique.

For notational convenience let $\mathbf{u}_\psi$ denote a control obtained by repeatedly applying Eq. (12) to $\mathbf{u}$ until the terminal constraints are satisfied. The proposed technique is that a one-dimensional minimization of J be performed with respect to θ_i, where $\mathbf{u}_{i+1}(t) = (\mathbf{u}_i + \theta_i \mathbf{p}_i)_\psi$. This necessitates the use of a one-dimensional minimization routine requiring only function value information. This procedure has theoretical justification since convergence proofs of conjugate direction gradient methods for problems with linear dynamics and quadratic performance index require a one-dimensional minimization at each step. Since more general optimal control problems can often be approximated by a linear-quadratic problem near the minimum, this algorithm should have some inherent advantages over algorithms not employing a one-dimensional minimization.

The proposed algorithm can be stated then as: 1) selection of an estimate $\mathbf{u}_0(t)$ of the optimal control; 2) projection of $\mathbf{u}_0(t)$ back to the constraint using Eq. (12), i.e., until $\|\boldsymbol{\psi}\| < \varepsilon$, for specified $\varepsilon > 0$; 3) letting $\mathbf{p}_i = -\tilde{H}_{u_i}{}^T$ (steepest descent); 4) choosing θ_i such that $J\{[\mathbf{u}_i(t) + \theta_i \mathbf{p}_i(t)]_\psi\}$ as a function of θ_i is a minimum; 5) setting $\mathbf{u}_{i+1}(t) = [\mathbf{u}_i(t) + \theta_i \mathbf{p}_i(t)]_\psi$; and 6) repeating items 3–5 until convergence is obtained.

Numerical Example

All computations were performed on an IBM 360/65 computer using double precision arithmetic. All integrations were performed using a standard 4th-order Runge-Kutta program with the time-

Table 1 Convergence history

Iteration number	Value of cost functional J	$\int_{t_0}^{t_f} \tilde{H}_u \tilde{H}_u^T dt$	$u(0)$	$u(0.5)$	$u(1)$
0	−4.07436	4.1196	$\pi/2$	$\pi/4$	0
0_ψ	−3.29834	9.5861	1.571	0.946	−0.932
1	−3.49072	0.7171	1.295	1.092	−1.032
2	−3.50696	0.0312	1.383	1.053	−0.994
3	−3.50781	0.0077	1.357	1.042	−0.984
4	−3.50800	0.0022	1.374	1.038	−0.979
5	−3.50806	0.0008	1.363	1.036	−0.978
Optimal[7]	−3.50809	0	1.367	1.034	−0.976

interval divided into 100 uniform segments. A quadratic polynomial approximation scheme was used for each one-dimensional minimization.

As a numerical example, consider the rocket problem treated in Ref. 7. In normalized form the 3rd-order dynamical system is

$$\dot{x}_1 = x_2, \quad x_1(0) = 0, \quad x_1(1) = 1.0$$
$$\dot{x}_2 = 6.4 \sin u - 3.2, \quad x_2(0) = 0, \quad x_2(1) = 0$$
$$\dot{x}_3 = 6.4 \cos u, \quad x_3(0) = 0$$

and the cost functional is $J = -x_3(1)$.

The convergence history obtained by using the proposed algorithm is given in Table 1. The iteration number 0_ψ refers to the control $[u_0(t)]_\psi$, where the initial control $u_0(t) = (\pi/2)(1-t)$. Since the differential equations of this problem are linear in the state variables, the transition matrix was calculated analytically, thus eliminating any numerical integration in the calculation[2] of the projection operator. The total execution time required for this solution was 19.2 sec. Figure 1 contains plots of $J[u_{i-1} + \theta_{i-1} p_{i-1}]$ and $J[(u_{i-1} + \theta_{i-1} p_{i-1})_\psi]$ vs the stepsize parameter θ_{i-1} for $i = 1, 5$. The $J(u)$ curves have lower minima since the constraints are violated. It should be noted that the minimum along the $J(u_\psi)$ curve is not in a region where the linearized dynamics are valid, thus lending support to the stepsize selection policy proposed by Willoughby.[6]

Conclusions

These numerical results demonstrate the feasibility of using this technique. The fact that this method is not dependent upon guessing additional algorithm parameters will hopefully make it a powerful tool in the future. The idea of using a one-dimensional minimization will be of greater importance when a conjugate gradient or Davidon algorithm is used since the generation of conjugate directions is highly dependent upon an accurate one-dimensional minimization. In light of the encouraging results resulting from using steepest descent on a rather simple problem, further investigation using a more advanced algorithm on a more sophisticated problem is warranted.

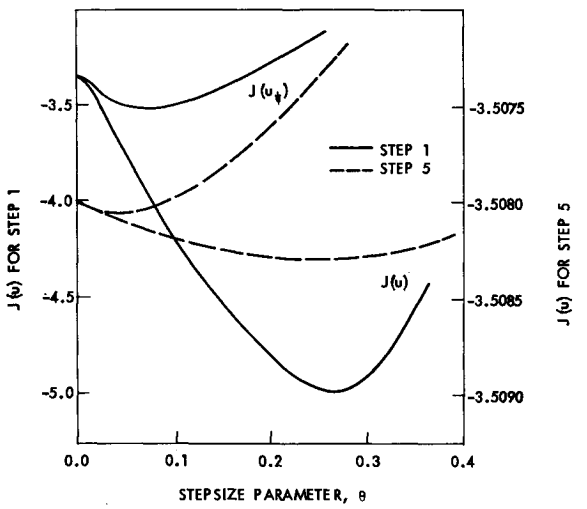

Fig. 1 One-dimensional search functional value profile.

References

[1] Bryson, A. E. and Ho, Y. C., *Applied Optimal Control*, Blaisdell, Waltham, Mass., 1969, pp. 39–41.

[2] Sinnott, J. F. Jr. and Luenberger, D. G., "Solution of Optimal Control Problems by the Method of Conjugate Gradients," *Proceedings of the Joint Automatic Control Conference*, American Automatic Control Council, 1967, pp. 566–574.

[3] Luenberger, D. G., *Optimization by Vector Space Methods*, Wiley, New York, 1969, Chap. 3.

[4] Horwitz, L. B. and Sarachik, P. E., "Davidon's Method in Hilbert Space," *SIAM Journal of Applied Mathematics*, Vol. 16, No. 4, July 1968, pp. 676–695.

[5] Mehra, R. K. and Bryson, A. E. Jr., "Conjugate Gradient Methods with an Application to V/STOL Flight-Path Optimization," *Journal of Aircraft*, Vol. 6, No. 2, March-April 1969, pp. 123–128.

[6] Willoughby, J. K., *Adaptations of the Conjugate Gradient Method to Optimal Control Problems with Terminal State Constraints*, TR ERI-62500, Feb. 1970, Engineering Research Inst., Ames, Iowa.

[7] Pierson, B. L., "A Discrete-Variable Approximation to Optimal Flight Paths," *Astronautica Acta*, Vol. 14, No. 2, Feb. 1969, pp. 157–169.

Solution of a Plastic Buckling Paradox

ARIS PHILLIPS*
Yale University, New Haven, Conn.

1. Introduction

IT is well known that the available experimental results on plastic buckling of plates and shells do not agree with a J_2-type flow theory but that they agree very well with a deformation-type theory or to a certain degree with a slip theory.[1,2] Taking into account that the deformation type theory as a class has been discredited because of inconsistencies[3] and that the slip theory has not been improved to an extent that it will satisfy experimental results,[4] it is worthwhile to show some new experimental results with yield surfaces because of their implications for solving this long standing problem of understanding plastic buckling.

The basis of the misunderstanding concerning plastic buckling may lie in the fact that it has not been recognized well experimentally that materials become anisotropic practically immediately upon plastic loading so that the use of an isotropic flow theory of plasticity is not appropriate particularly for the solution of problems in which the appearance of a very small plastic strain is of great importance; this is, of course, the case in plastic buckling.

2. New Experimental Results

Figures 1 and 2 show typical yield surfaces in a tension-torsion stress space as obtained experimentally for commercially pure aluminum. We shall assume that the same general results are valid for other metals and for other stress-space quadrants such as the compression-torsion space. Indeed initial isotropy requires that

Received January 7, 1972. The author would like to express his appreciation to the National Science Foundation for the support of this research under a grant to Yale University.

* Professor, Department of Engineering and Applied Science.